Journal of Experimental Nanoscience
Publication details, including instructions for authors and subscription information:
http://www.informaworld.com/smpp/title~content=t716100757

Crystallisation behaviour and morphological characteristics of poly(propylene)/multi-walled carbon nanotube nanocomposites

Amir Bahram Kaganj[ab]; Ali Morad Rashidi[b]; Rouhollah Arasteh[bc]; Sohrab Taghipoor[b]
[a] Department of Mechanical Engineering, Tarbiat Modares University, Tehran, Iran [b] Gas Research Division, Research Institute of Petroleum Industry (RIPI), Tehran, Iran [c] Department of Textile Engineering, Islamic Azad University, South Tehran Branch, Tehran, Iran

To cite this Article Kaganj, Amir Bahram , Rashidi, Ali Morad , Arasteh, Rouhollah and Taghipoor, Sohrab(2009) 'Crystallisation behaviour and morphological characteristics of poly(propylene)/multi-walled carbon nanotube nanocomposites', Journal of Experimental Nanoscience, 4: 1, 21 — 34
To link to this Article: DOI: 10.1080/17458080802688427
URL: http://dx.doi.org/10.1080/17458080802688427

Journal of Experimental Nanoscience
Vol. 4, No. 1, March 2009, 21–34

Taylor & Francis
Taylor & Francis Group

Crystallisation behaviour and morphological characteristics of poly(propylene)/multi-walled carbon nanotube nanocomposites

Amir Bahram Kaganj[ab], Ali Morad Rashidi[b]*, Rouhollah Arasteh[bc] and Sohrab Taghipoor[b]

[a]*Department of Mechanical Engineering, Tarbiat Modares University, Tehran, Iran;* [b]*Gas Research Division, Research Institute of Petroleum Industry (RIPI), Tehran, Iran;* [c]*Department of Textile Engineering, Islamic Azad University, South Tehran Branch, Tehran, Iran*

(*Received 8 July 2008; final version received 14 December 2008*)

The objectives of this article are to study the crystallisation behaviour and morphology of melt compounded nanocomposites of poly(propylene) (PP) and multi-walled carbon nanotubes (MWNTs). A PP matrix containing different contents of 0, 1, 2, 4 and 8 wt% of the MWNTs nanofiller was prepared for this investigation. Studies using a differential scanning calorimetry and a wide angle X-ray diffraction indicated that the MWNTs promoted heterogeneous nucleation. The nucleant of the MWNTs affected the crystallisation of the PP, but was not linearly dependent on the MWNT content which meant a saturation of the nucleant effect at low carbon nanotube content. The relative amount, crystallite size and distribution of different crystallites in the PP varied because of the addition of the MWNTs, which affected the final properties of the nanocomposites. Meanwhile, the degree of crystallinity of the PP exhibited an increasing trend with the addition of MWNTs, followed by moderate decreases at higher content. Continuous scanning electron microscopy observations indicate that the nanotubes are well dispersed in the PP matrix at low content of MWNTs. Each nanotube is covered by a layer of PP molecules.

Keywords: poly(propylene); multi-walled carbon nanotubes; crystallisation; nanocomposites

1. Introduction

Since Ijiima discovered carbon nanotubes (CNTs) by arc discharge method in 1991 [1], extensive studies have been devoted to the use of CNTs as nanofillers, because of their unusual mechanical and electrical properties, to improve the performance of a matrix or to achieve new properties [2,3]. One of the advantages of CNTs as a reinforcement is their large surface area that can induce a better adhesion with the polymeric matrix, which is an important factor for effective enhancement of the composite properties, such as temperature, solvent resistance, crystallinity, microstructure, thermal expansion coefficient, dielectric constant, mechanical properties, and so on [4–17].

*Corresponding author. Email: rashidiam@ripi.ir

ISSN 1745–8080 print/ISSN 1745–8099 online

DOI: 10.1080/17458080802688427
http://www.informaworld.com

Polyolefins, such as poly(propylene) (PP), are among the most versatile polymer matrices, and are very widely used because of their good balance between properties and cost, as well as their nice processability and low density. However, the mechanical and thermal properties are not sufficient for applications as engineering plastics. Therefore, PP is generally modified by melt mixing with nano-scaled clay [18–22] and fibres. Recently, CNTs were also used as special nanofiller to prepare PP/CNT nanocomposites, which provide a new way to obtain high-performance PP engineering plastics. Many physical properties, such as crystallisation behaviour, mechanical properties, morphology, thermal behaviour, and conductivity of PP/CNT nanocomposites were hence studied extensively [23–30].

Some common methods for the preparation of polymer/CNT nanocomposites include: *in-situ* polymerisation [31,32], solution mixing [33–34] and melt blending [35–37]. The composite prepared by the first two methods may result in contamination because of the residual monomer or solvent. However, those prepared by melt blending are essentially free of such contamination. In addition, the tendency of CNTs to form aggregates may be minimised by appropriate application of shear during melt mixing [38,39].

The crystallisation behaviour and morphology development under isothermal and nonisothermal conditions of PP reinforced with single-walled carbon nanotubes (SWNTs) have been reported by Valentini et al. [25,26], Bhattacharyya et al. [27], and Leelapornpisit et al. [28], and PP reinforced with multi-walled carbon nanotubes (MWNTs) has been researched by Assouline et al. [7,24], and Seo et al. [30], and etc.

In PP matrix nanocomposites, the presence of reinforcements influences the crystalline morphology of PP as they act as nucleating agents. Because the crystalline morphology will affect the mechanical properties of PP nanocomposites, an investigation of crystallisation phenomena is of great importance. Compared with the traditional inorganic fillers, CNTs have a unique atomic structure and a very high aspect ratio, which can act as a strong nucleation agent for PP matrix.

In this work, we investigated the effects of different concentrations of MWNTs on the crystalline kinetics and morphology of PP matrix nanocomposites. The thermal characterisation was performed by differential scanning calorimetry (DSC). The structural properties of the nanocomposites at several MWNTs concentrations have been studied by scanning electron microscopy (SEM).

2. Experimental

2.1. *Materials*

The PP used in this study was of extrusion grade PI0800 (melt flow index (MFI) 7–10 g/10 min at 190°C under 2.16 Kg), obtained from Bandar Imam Petrochemical Co. (Iran). MWNTs were prepared by chemical vapour deposition (provided by Research Institute of Petroleum Industry, RIPI) with diameters ranging from 10 to 50 nm, lengths varying from 1 to 3 μm and purity of 96%. The TEM of MWNT used for nanocomposites preparation is shown in Figure 1. The MWNTs were dispersed on 2-propanol and then the product was examined by a transmission electron microscope (TEM on a CM 120 Philips with a tension voltage of 120 kV).

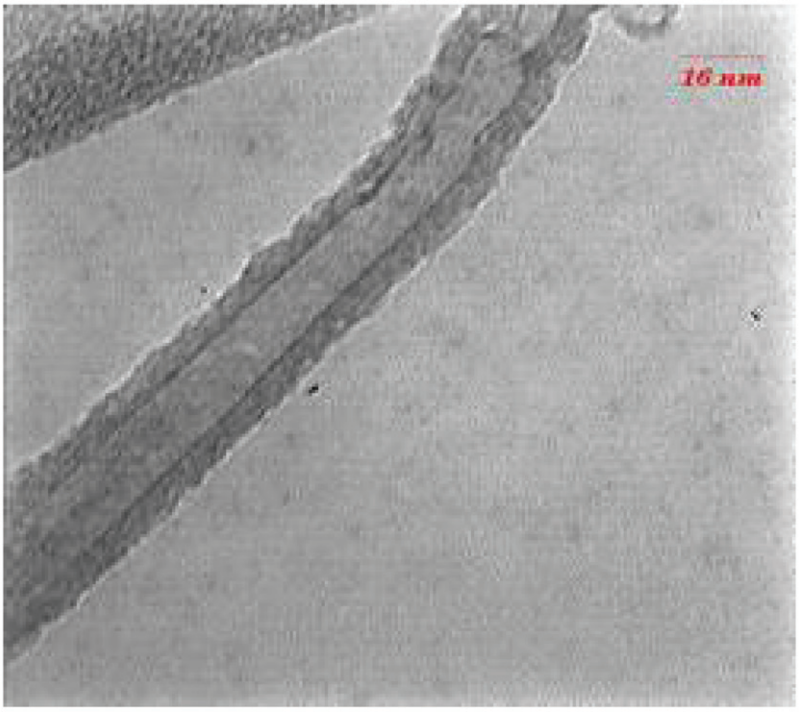

Figure 1. TEM image of MWNT.

Table 1. Compositions of PP/MWNT nanocomposites.

Sample code	PP (wt%)	MWNT (wt%)
NC0	100	0
NC1	99	1
NC2	98	2
NC3	96	4
NC4	92	8

2.2. *Preparation of MWNT/PP nanocomposites*

The PP/MWNT nanocomposites having various MWNT content are listed in Table 1. These nanocomposites were prepared by melt blending of MWNT and PP pellets in a Brabender internal mixer with roller-type rotors operating at 190°C and 60 rpm. As shown in Table 1, the minor phase content (MWNT) was varied between 0 and 8%. Compounds were carried out by first feeding PP into the mixer and, after 3 min mixing and melting of PP pellets, charging a specified amount of MWNTs into the mixer. Mixing was continued for 12 min. When the torque of the mixer became constant, the composite was deemed complete. The maximum duration of the mixing period

would be 15 min. 2 and 3 mm sheets were prepared by compression molding under a pressure of about 150 bar at 200°C for 5 min using a hydraulic press.

2.3. *Scanning electron microscopy (SEM)*

Morphologies of the nanocomposites were studied using a SEM (SEM XL 30; Philips Instruments). SEM micrographs were taken from cryogenically fractured surfaces of compression-molded specimens. The sheets were fractured manually after immersion in liquid nitrogen and were then coated with a thin layer of gold prior to SEM investigation.

2.4. *Differential scanning calorimetry (DSC)*

Crystallisation behaviour was studied using a DSC model Stanton Redcraft STA-780 (London, UK). Indium was used for temperature calibration ($T_m = 156.6$°C, $\Delta H_m = 28.4\,J\,g^{-1}$). All the samples were dried prior to the measurements and analyses were done in a nitrogen atmosphere using standard aluminum pans. Calorimetric measurements were done while the samples (4–5 mg) were exposed to the following temperature scans: heating at a rate of 10°C$\,min^{-1}$ to 240°C, holding for 10 min to erase thermal history effects and then cooling to −30°C at a rate of 10°C$\,min^{-1}$ during which the peak of crystallisation exotherm was taken as the crystallisation temperature, T_C. Then the samples were reheated to 240°C at a rate of 10°C$\,min^{-1}$ to observe the subsequent melting behaviour. The heat of fusion (ΔH_m) and the heat of crystallisation (ΔH_c) were determined from the areas of the melting and crystallisation peaks, respectively.

2.5. *Wide angle X-ray diffraction (WXRD)*

To evaluate the average crystal size of the PP nanocomposites, WXRD was performed with a Philips Analytical X-ray using nickel-filtered Cu-Kα radiation ($\lambda = 0.15406$ nm) under a voltage of 40 kV and a current of 25mA. The WXRD patterns were recorded with a step size of 0.05° from $2\theta = 1$–40°.

3. Results and discussion

3.1. *Morphology of PP nanocomposites*

In Figure 2, the fracture surface morphology of 1, 2, 4 and 8 wt% PP/MWNTs nanocomposites, investigated by SEM analysis, are shown. The white spots indicate MWNT's ends that were pulled out of the polymer matrix. Although we observed small quantity of aggregates at the concentration of 1 wt% MWNT's, a more uniform distribution of the bundles was taken in nanocomposites with a low amount of MWNTs (Figure 2(b)).

As can be seen in Figures 2(e) and (f), the propensity of aggregation of MWNTs grows with the increasing MWNT content. For the concentration of 8% we can see an aggregate in which we observe a large amount of MWNTs self-organised in bundles. At high MWNT content it is clear from the micrographs that the dispersion of MWNTs in the PP matrix is not perfect and more agglomerates of MWNTs form in PP matrix and many

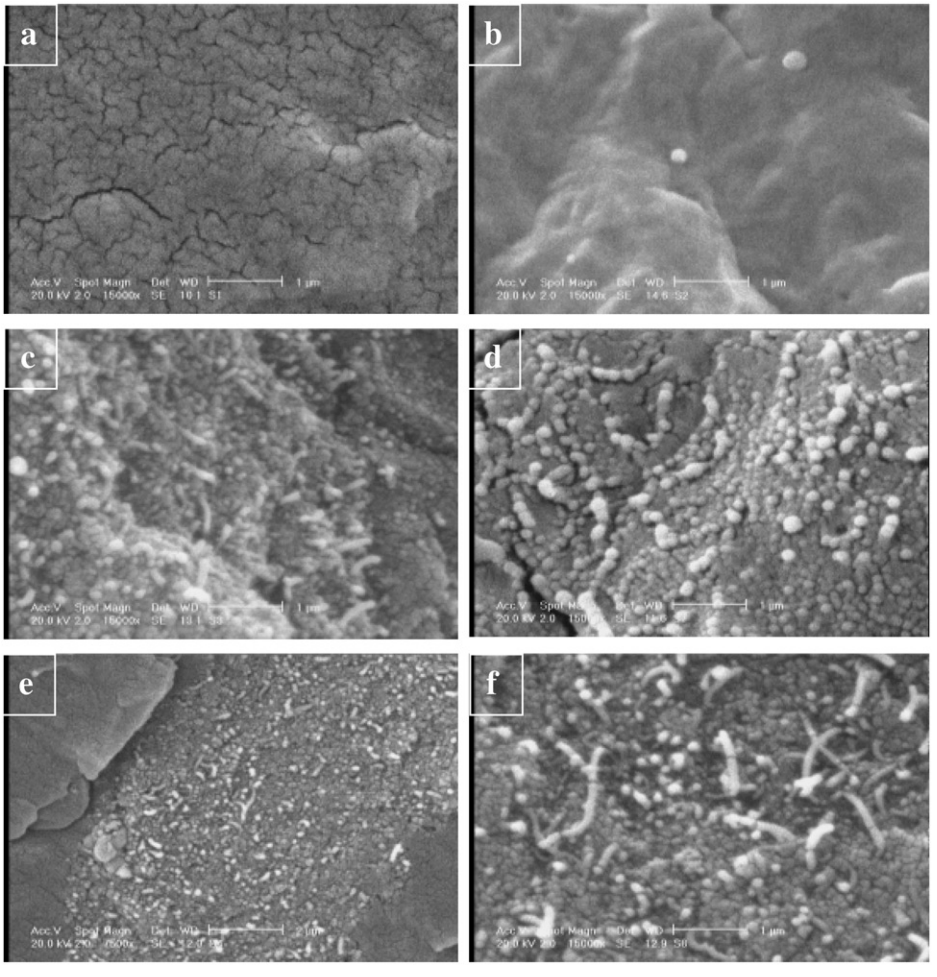

Figure 2. SEM images of cryogenically fractured surfaces of compression molded sheets: (a) NC0, (b) NC1, (c) NC2, (d) NC3 and (e) and (f) NC4. (a), (b), (c), (d), (f) in 15,000X, (e) in 7500X magnification.

defects are introduced into polymer matrix. In some areas the concentration of MWNTs is high, but none of MWNTs can be found in some other areas. It can be found that approximately micrometre diameter clusters of MWNTs appear in partial areas. Though high shear force and mixing energy are produced during melt mixing, MWNTs agglomerates can still withstand high shear force and remain entangled. This can be ascribed to the strong intermolecular Van-der Waal's interactions among the nanotubes and the poor interfacial interactions between MWNTs and PP matrix result in the poor dispersion of MWNTs in PP matrix. When the MWNT content reaches 8 wt% compared with the 1 wt% PP/MWNTs nanocomposites, more MWNTs are entangled with each other and the diameter of MWNT clusters is larger. These defects lead to a decrease in tensile strength.

3.2. *Crystallisation characteristics*

The effects of MWNTs on the crystallisation characteristics of melt compounded PP/MWNTs nanocomposite samples were analysed first with non-isothermal DSC experiments. From the DSC crystallisation exotherms recorded as the samples were crystallised in the molten state at a given cooling rate, some useful parameters can be obtained to describe the non-isothermal crystallisation. These parameters are defined below and illustrated in Figure 3.

T_p: The peak temperature of crystallisation exotherm.

T_C: is the temperature at the intercept of the tangents at the baseline and the high-temperature side of the exotherm.

$T_C - T_p$: The inverse measure of the overall rate of crystallisation. The smaller the $T_C - T_p$, the greater the rate of crystallisation is.

S_i: Slope of initial portion of the exotherm, which is a measure of the rate of nucleation. The greater the initial slope, the faster the nucleation rate is.

ΔW: The width at half-height of the exotherm peak determined after normalisation of the peak to a constant mass of the samples, which is a measure of the crystallite size distribution. The narrower the crystallite size distribution, the smaller will be ΔW.

T_P, T_C, $T_C - T_p$, ΔH and ΔW were obtained and are listed in Table 2.

An increase in the crystallisation temperature of the PP with the addition of MWNTs was indicated (Table 3 and Figure 4). All the T_p values of the nanocomposite samples are higher than that of pure PP (109°C) and T_p increases with increasing MWNTs weight. At low MWNT content (1 wt%), T_p increases dramatically. However, after MWNTs loading reaches 2 wt%, T_p values of the PP nanocomposite samples increase slightly. At a MWNT content of 1wt%, T_p is increased by 12.3°C with respect to that of PP. This phenomenon

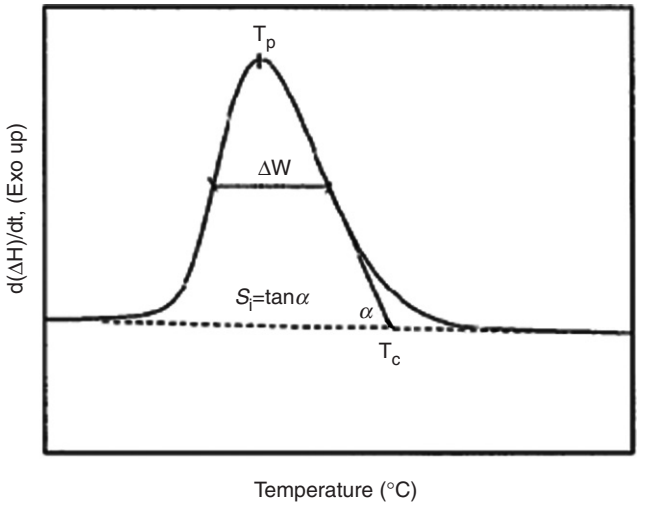

Figure 3. Schematic representation of the non-isothermal crystallisation parameters determined from DSC crystallisation exotherm.

is attributed to the fact that MWNTs act as a nucleating agent to promote faster crystal growth and the creation of a large number of smaller spherulites in a heterogeneous nucleation process. When the loading of MWNTs is increased, there is a saturation of the nucleant effect at low MWNT concentrations, resulting in diminishing dependence on the increasing MWNTs-induced nucleation, possibly because of the large surface area and good dispersion of MWNTs. As a result, the crystallisation temperature increases by the addition of MWNTs. All the $T_C - T_P$ values of the nanocomposite samples are smaller than that of pure PP, indicating that the addition of MWNTs into PP increased the overall rate of crystallisation of PP.

The parameters of the rate of nucleation (S_i) and the width at half-height of the exotherm peak (ΔW) are also listed in Table 2. The S_i of all PP nanocomposite samples

Table 2. Non-isothermal crystallisation parameters of PP and PP/MWNT nanocomposites in the cooling process.

Sample	T_p (°C)	T_c (°C)	$T_C - T_p$	ΔH_c (W/g^{-1})	S_i	ΔW (°C)
NC0	109	116.2	7.2	97.39	6.31	8.55
NC1	121.3	125.6	4.3	101.9	14.3	5.26
NC2	122.1	128.3	6.2	95.25	7.12	5.92
NC3	123.5	130.1	6.6	94.09	8.14	5.96
NC4	126.5	131.9	5.4	90.31	8.14	6.58

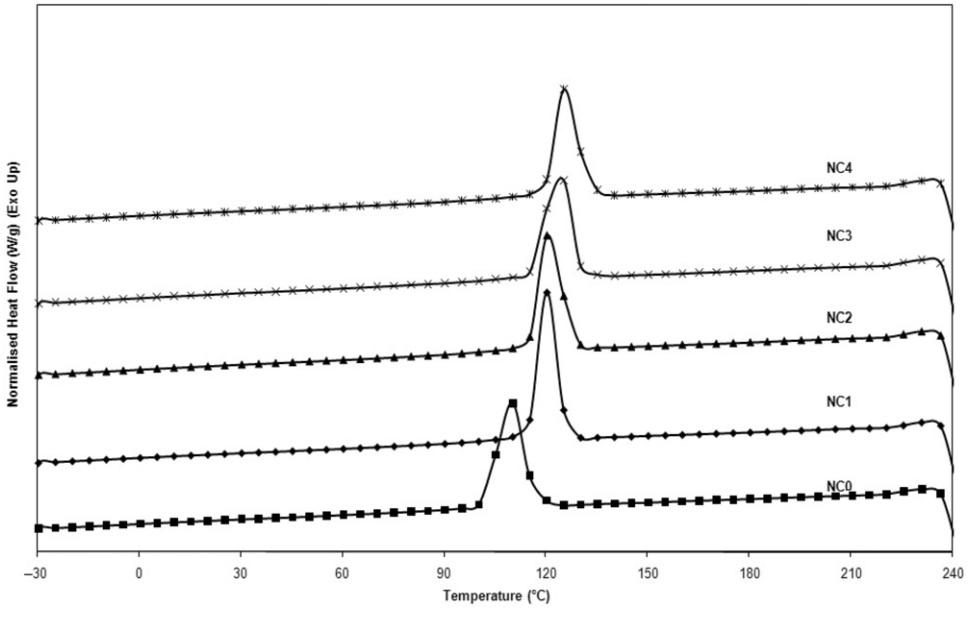

Figure 4. DSC cooling scans (10°C min^{-1} from 240°C melt) of PP/MWNT nanocomposites samples.

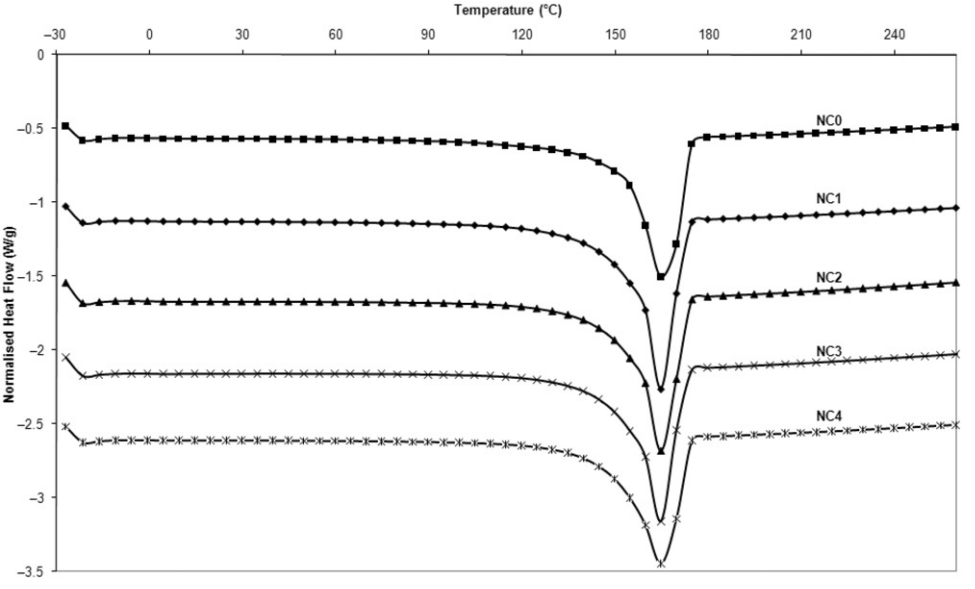

Figure 5. DSC heating scans of PP/MWNT nanocomposites samples.

are greater than that of pure PP, implying that the PP nanocomposites have higher rate of nucleation. When MWNT content reaches 1 wt%, the S_i of PP attains the greatest value.

ΔW of all PP/MWNTs nanocomposites are smaller than that of neat PP, implying that the PP/MWNTs nanocomposites have more uniform crystallite size distribution. ΔW of 1 wt% MWNTs-filled PP dramatically decreases with respect to that of PP. Increasing MWNT content results in the slight increase of ΔW, indicating that the crystallite size distribution in the PP nanocomposites is narrower than that of neat PP. However, a limiting effect of crystallisation nuclei may be reached after the addition of 1 wt% of MWNTs.

Analysis of the data in Table 2 shows that MWNTs can act as effective nucleating agents, increasing the peak temperature and the overall rate of the crystallisation of PP. The rate of nucleation and narrow crystallite size distribution of PP increased with the addition of MWNTs.

The DSC thermogram for the second heating process is shown in Figure 5. The peak temperature of crystallisation melting (T_m) and the melting heat of crystallisation (ΔH_m) are listed in Table 3. The crystalline fraction of the composites, X_c, was calculated from:

$$X_c = \frac{\Delta H_m}{\Delta H_0} \times 100 \quad (1)$$

Where the melting enthalpy of a 100% crystalline PP, $\Delta H_0 = 207.1\ \mathrm{W\,g^{-1}}$.

From these results, the degree of supercooling (the difference in the melting peak temperature and crystallisation peak temperature) was obtained.

As can be seen, the peak temperature of crystallisation melting, T_m, was almost independent of MWNTs loading. The degree of supercooling of specimens decreased with

Table 3. Non-isothermal crystallisation parameters of PP and PP/MWNT nanocomposites in the heating process.

Sample	T_m (°C)	$T_m - T_p$	ΔH_m (W g^{-1})	X_c (%)
NC0	166.4	57.4	97.21	46.96
NC1	165.3	44	105.1	50.77
NC2	165.9	43.8	98.8	47.73
NC3	165.4	41.9	98.2	47.44
NC4	166.1	39.6	95.35	46.06

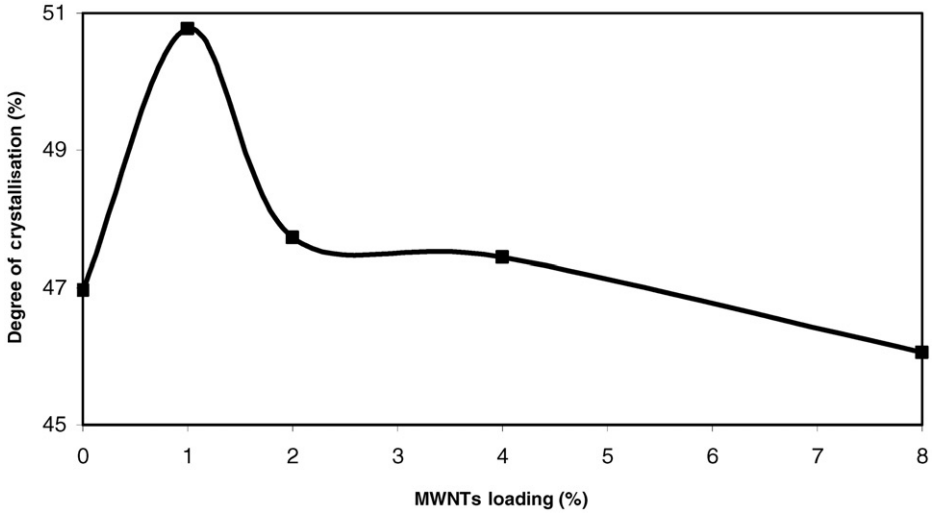

Figure 6. Degree of crystallisation versus weight fraction of MWNTs for PP nanocomposites.

increasing MWNTs loading in the matrix, which indicates more perfect crystallisation can occur in PP nanocomposites.

The calculated degree of crystallinity of specimens exhibited an increased trend with increasing content of MWNTs, followed by a moderate decrease at higher content. As shown in Figure 5 and Table 3, the crystalline fraction increased from 47% for neat PP matrix to 50.77% for 1 wt% PP/MWNT nanocomposites and then in higher loading of MWNTs, degree of crystallisation is decreased. This phenomenon implies that nanotubes dispersed in the PP promoted heterogeneous nucleation as the MWNTs were added into the PP matrix. On the other hand, when the loading of the nanotubes is small, the mobility of the PP macromolecular chains can be enhanced. Thus, the crystallisation rate and degree of crystallinity of the specimens increased.

When the content of nanotubes increased, the fillers started to block the mobilisation of the PP macromolecular chains and prevent macromolecular segments from obtaining order alignment of crystal lattices. As shown in Figure 6, the degree of crystallinity of

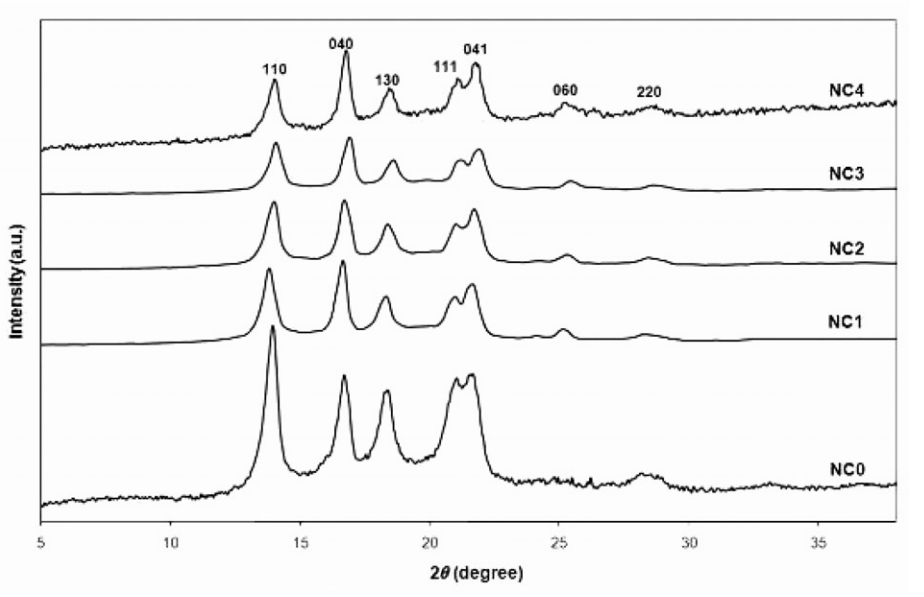

Figure 7. WXRD patterns of PP/MWNTs nanocomposites.

specimens increased sharply in 1 wt% PP/MWNT nanocomposites and then decreased at high MWNT content.

3.3. *Crystal structure of PP nanocomposites*

The WXRD has been used to investigate the crystalline structure of PP and PP/MWNTs nanocomposite. Figure 7 shows the WXRD intensity profiles of PP and PP/MWNTs nanocomposite. It is well known that the PP mainly exhibits three crystalline forms: monoclinic α, trigonal β, and triclinic γ, depending on the crystallisation conditions. Seven strong peaks at $2\theta = 13.88$, 16.68, 18.42, 21, 21.69, 25.19, and 28.36° corresponding, respectively to [110], [040], [130], [111], [041], [060], and [220] planes can be seen in the integrated XRD intensity of PP/MWNTs nanocomposite, indicating the existence of typical α-form PP crystals and the absence of β-form crystals. This study shows only the α-crystal formation in PP/MWNT nanocomposites, and it can be concluded that MWNTs can not affect the crystalline polymorph of PP.

The space between the different diffraction planes of the α-form crystals (d_{hkl}) can be obtained by the Bragg Equation:

$$d_{hkl} = \frac{n\lambda}{2\sin\theta_{hkl}} \tag{2}$$

where n is the diffraction level, λ is the wavelength of X-rays and θ_{hkl} is the Bragg angle.

The crystallite size (L_{hkl}) in the direction perpendicular to the set of lattice planes can be obtained using the Scherrer Equation:

$$L_{hkl} = \frac{k\lambda}{\beta_{hkl}\ cos\theta_{hkl}} \tag{3}$$

Table 4. Structural parameters of α-form crystals for PP nanocomposites.

Sample	Diffraction peak	2θ / °	d_{hkl} / Å	β_{hkl}	L_{hkl} / nm
NC0	110	13.88	6.38	0.01	13.97
	040	16.68	5.31	0.01136	12.34
	130	18.42	4.81	0.01514	9.28
	111	21	4.23	0.01388	10.16
	041	21.69	4.09	0.01262	11.19
	060	25.19	3.53	0.0096	14.8
	220	28.36	3.14	0.0202	7.08
NC1	110	13.80	6.34	0.0103	13.56
	040	16.63	5.31	0.00854	16.41
	130	18.31	4.81	0.0123	11.42
	111	21	4.23	0.0125	11.28
	041	21.71	4.09	0.0120	11.77
	060	25.29	3.52	0.01	14.21
	220	28.27	3.13	0.0178	8.03
NC2	110	13.96	6.34	0.0103	13.56
	040	16.83	5.27	0.00981	14.29
	130	18.44	4.81	0.0125	11.23
	111	21.02	4.22	0.0123	11.47
	041	21.76	4.08	0.0120	11.77
	060	25.36	3.51	0.0101	14.07
	220	28.34	3.15	0.0158	9.05
NC3	110	14.07	6.29	0.01009	13.97
	040	16.79	5.27	0.0096	14.6
	130	18.38	4.82	0.0116	12.1
	111	21.02	4.22	0.0111	12.7
	041	21.78	4.08	0.0123	11.47
	060	25.27	3.52	0.01034	13.8
	220	28.45	3.14	0.0148	9.66
NC4	110	13.97	6.34	0.008834	15.81
	040	16.76	5.29	0.00883	15.87
	130	18.43	4.81	0.01136	12.36
	111	21.02	4.22	0.0106	13.3
	041	21.89	4.06	0.0123	11.48
	060	25.27	3.52	0.0176	8.07
	220	28.46	3.13	0.0151	9.47

where k is the shape factor of the crystallites (taken as 0.9 here), and β_{hkl} is the broadening of diffraction peaks, which is related to the width at half height of the diffraction peak (unit of radians).

The structural parameters of α-form crystals in PP nanocomposites were obtained from the WXRD patterns and are listed in Table 4. From the data shown in Table 4, it was found that there was no obvious shift of all the diffraction peak positions. Therefore, the addition of MWNTs had a negligible influence on the distance between the diffraction planes of crystallites in the PP. Meanwhile, the intensity and width of some diffraction

peaks changed, arising from the addition of MWNTs. The relative amount of diffraction peaks corresponding to the [110] and [111] crystal planes of the α-form decreased with increasing MWNT loading, and the crystallite size in the direction perpendicular to the set of lattice planes also reduced. At the same time, the intensity and relative amount of diffraction peaks corresponding to the [040] and [060] crystal plane of the α-form was enhanced with increased loading of MWNTs. The addition of MWNTs brought an increase in crystallite size of the [040] crystal plane, but induced lessening of the crystallite size of the [060] crystal plane.

4. Conclusions

This report describes the fabrication of a range of PP/MWNT nanocomposites and, in particular, the impact of CNTs on the crystallisation and morphological behaviour of a PP matrix. The crystallisation temperature of the PP matrix is increased with the addition of MWNTs, while the melting temperature was independent of MWNT content. The degree of crystallinity of PP exhibited an increased trend with enhanced content of MWNTs, followed by a moderate decrease at higher content. MWNTs can act as nucleating agents using melt processing technique. MWNTs supplies heterogeneous nuclei and make the process of nuclei formation rapidly finished, which suggested that MWNTs plays a role of nucleating agent. The results show that the addition of CNTs accelerates the overall non-isothermal crystallisation process of PP.

Also, the integrated WXRD intensity of the composites showed the typical α-form PP crystals and exhibited complete absence of the β-crystal form.

Scanning electron micrographs shows that both individual MWNTs and agglomerations of MWNTs can be observed even at the low content of 1 wt%. The tendency of agglomeration of MWNTs is improved with the increasing MWNTs content. The morphology observed by microscopy confirms the thermal analysis results concerning the positive effects of low MWNTs concentrations on nucleation and crystallisation kinetics.

References

[1] S. Iijima, *Helical mircotubles of graphitic carbon*, Nature 354 (1991), pp. 56–58.
[2] R. Andrews and M.C. Weisenberger, *Carbon nanotube polymer composites*, Curre. Opin. Sol. St. Mat. Sci. 8 (2004), pp. 31–37.
[3] S.P. Bao and S.C. Tjong, *Mechanical behaviors of polypropylene/carbon nanotube nanocomposites: The effects of loading rate and temperature*, Mat. Sci. Eng. A. 485 (2008), pp. 508–516.
[4] Z. Yaping, Z. Aibo, C. Qinghau, Z. Jiaoxia, and N. Rongchang, *Functionalized effect on carbon nanotube/epoxy nanocomposites*, Mat. Sci. Eng. A. 145 (2006), pp. 435–436.
[5] K.P. Ryan, M. Cadek, V. Nicolosi, D. Blond, M. Ruether, G. Armstrong, H. Swan, A. Fonseca, J.B. Nagy, W.K. Maser et al., *Carbon nanotubes for reinforcements of plastics? A case study with poly(vinyl alcohol)*, Comp. Sci. Tech. 67 (2007), pp. 1640–1649.
[6] B.P. Grady, F. Pompeo, R.L. Shambaugh, and D.E. Resasco, *Nucleation of polypropylene crystallization by single-walled carbon nanotubes*, J. Phys. Chem. B 106 (2002), pp. 5852–5858.
[7] E. Assouline, A. Lustiger, A.H. Barber, C.A. Cooper, E. Klein, E. Wachtel, and H.D. Wagner, *Nucleation ability of multiwall carbon nanotubes in polypropylene composites*, J. Polym. Sci. Part B: Polym. Phys. 41 (2003), pp. 520–5277.

[8] W. Leelapornpisit, M.T. Ton-That, F. Perrin-Sarazin, K.C. Cole, J. Denault, and B. Simard, *Effect of carbon nanotubes on the crystallization and properties of polypropylene*, J. Polym. Sci. Part B. 43 (2005), pp. 2445–2453.
[9] Z. Zhou, S.F. Wang, L. Lu, Y. Zhang, and Y.X. Zhang, *Isothermal crystallization kinetics of polypropylene with silane functionalized multi-walled carbon nanotubes*, J. Polym. Sci. Part B: 45 (2007), pp. 1616–1624.
[10] K. Wang, C.Y. Tang, P. Zhao, H. Yang, Q. Zhang, R.N. Du, and Q. Fu, *Rheological investigations in understanding shear-enhanced crystallization of isotactic poly(propylene)/multi-walled carbon nanotube composites*, Macromol. Rapid. Commun. 28 (2007), pp. 1257–1264.
[11] H. Zhang and Z. Zhang, *Impact behaviour of polypropylene filled with multi-walled carbon nanotubes*, Euro. Polym. J. 43 (2007), pp. 3197–3207.
[12] Y. Xiao, X.Q. Zhang, W. Cao, K. Wang, H. Tan, Q. Zhang, R.N. Du, and Q. Fu, *Dispersion and mechanical properties of polypropylene/multiwall carbon nanotubes composites obtained via dynamic packing injection molding*, J. Appl. Polym. Sci. 104 (2007), pp. 1880–1886.
[13] P. Zhao, K. Wang, H. Yang, Q. Zhang, R.N. Du, and Q. Fu, *Excellent tensile ductility in highly oriented injection-molded bars of polypropylene/carbon nanotubes composites*, Polymer 48 (2007), pp. 5688–5695.
[14] M. Ganb, B.K. Satapathy, M. Thunga, R. Weidisch, P. Potschke, and A. Janke, *Temperature dependence of creep behavior of PP-MWNT nanocomposites*, Macromol. Rapid. Commun. 28 (2007), pp. 1624–1633.
[15] C.A. Avila-Orta, F.J. Medellin-Rodriguez, M.V. Davila-Rodriguez, Y.A. Aguirre-Figueroa, K. Yoon, and B.S. Hsiao, *Morphological features and melting behavior of nanocomposites based on isotactic polypropylene and multiwalled carbon nanotubes*, J. Appl. Polym. Sci. 106 (2007), pp. 2640–2647.
[16] M.V. Jose, D. Dean, J. Tyner, G. Price, and E. Nyairo, *Polypropylene/carbon nanotube nanocomposite fibers: Process-morphology-property relationships*, J. Appl. Polym. Sci. 103 (2007), pp. 3844–3850.
[17] B.B. Marosfi, A. Szabo, G. Marosi, D. Tabuani, G. Camino, and S. Pagliari, *Linear viscoelastic properties and crystallization behavior of multi-walled carbon nanotube/polypropylene composites*, J. Therm. Anal. Cal. 86 (2006), p. 669.
[18] M. Kawasumi, N. Hasegawa, M. Kato, A. Usuki, and A. Okada, *Preparation and mechanical properties of polypropylene-clay hybrids*, Macromolecules 30 (1997), pp. 6333–6338.
[19] M.J. Solomon, A.S. Almusallam, K.F. Seefeldt, A. Somwangthanaroj, and P. Varadan, *Rheology of polypropylene/clay hybrid materials*, Macromolecules 34 (2001), pp. 1864–1872.
[20] J. Li, C.X. Zhou, G. Wang, and D.L. Zhao, *Study on kinetics of polymer melt intercalation by a rheological approach*, J. Appl. Polym. Sci. 89 (2003), pp. 318–323.
[21] L.J. Zhao, J. Li, S.Y. Guo, and Q. Du, *Ultrasonic oscillations induced morphology and property development of polypropylene/montmorillonite nanocomposites*, Polymer 47 (2006), p. 2460.
[22] J. Li, M.T. Ton-That, W. Leelapornpisit, and L.A. Utracki, *Melt compounding of polypropylene-based clay nanocomposites*, Polym. Eng. Sci. 47 (2007), p. 1447.
[23] C.M. Wu, M. Chen, and J. Karger-Kocsis, *Micromorphologic feature of the crystallization of isotactic polypropylene after melt-shearing*, Polymer Bulletin 41 (1998), pp. 493–499.
[24] E. Assouline, S. Pohl, R. Fulchiron, J.F. Gerard, A. Lustiger, H.D. Wagner, and G. Marom, *The kinetics of α and β transcrystallization in fibre-reinforced polypropylene*, Polymer 21 (2000), pp. 7843–7854.
[25] L. Valentini, J. Biagiotti, J.M. Kenny, and S. Santucci, *Morphological characterization of single-wall carbon nanotube/polypropylene composites*, Compos. Sci. Technol. 63 (2003), pp. 1149–1153.
[26] L. Valentini, J. Biaqiotti, M.A. Lopez-Manchado, S. Santucci, and J.M. Kenny, *Effects of single-walled carbon nanotubes on the crystallization behavior of polypropylene*, J. Appl. Polym. Sci. 87 (2003), pp. 708–713.

[27] A.R. Bhattacharyya, T.V. Sreekumar, T. Liu, S. Kumar, L.M. Ericson, R.H. Hauge, and R.E. Smalley, *Crystallization behavior of polypropylene/single-wall carbon nanotube composites*, Polymer 44 (2003), pp. 2373–2377.

[28] W. Leelapornpisit, M. Ton-That, F. Perrin-Sarazin, K.C. Cole, J. Denault, and B. Simard, *Effect of carbon nanotubes on the crystallization and properties of polypropylene*, J. Polym. Sci. Part B: Polym. Phys. 43 (2005), p. 2445.

[29] T.E. Chang, L.R. Jensen, A. Kisliuk, R.B. Pipes, R. Pyrz, and A.P. Sokolov, *Microscopic mechanism of reinforcement in single wall carbon nanotube/polypropylene nanocomposites*, Polymer 46 (2005), pp. 439–444.

[30] M.K. Seo, J.R. Lee, and S.J. Park, *Crystallization kinetics and interfacial behaviors of polypropylene composites reinforced with multi-walled carbon nanotubes*, Mater. Sci. Eng. A. 404 (2005), pp. 79–84.

[31] Z. Wang, M. Lu, H.L. Li, and X.Y. Guo, *SWNTs/polystyrene composites preparations and electrical properties research*, Mat. Chem. Phys. 100 (2006), pp. 77–81.

[32] J. Xiong, Z. Zhang, X. Qin, M. Li, and X. Wang, *The thermal and mechanical properties of a polyurethane/multi-walled carbon nanotubes composite*, Carbon 44 (2006), pp. 2701–2707.

[33] K.P. Ryan, M. Cadek, V. Nicolosi, S. Waller, M. Ruether, A. Fonseca, J.B. Nagy, W.T. Blan, and J.N. Coleman, *Multiwalled carbon nanotube nucleated crystallization and reinforcement in poly(vinyl alcohol) composites*, Synth. Meta. 156 (2006), pp. 332–335.

[34] L. Qu, Y. Lin, D.E. Hill, and B. Zhou, *Polyimide-functionalized carbon nanotubes: Synthesis and dispersion in nanocomposite films*, Macromolecules 37 (2004), p. 6055.

[35] S.L. Ryan, P. Gao, X.G. Yang, and T.X. Yu, *Toughening high performance ultra high molecular weight polyethylene using multiwalled carbon nanotubes*, Polymer 44 (2003), pp. 5643–5654.

[36] Q. Zhang, S. Rastogi, D. Chen, D. Lippits, and P.J. Lemstra, *Low percolation threshold in single walled carbon nanotube/high-density polyethylene composites prepared by melt-processing technique*, Carbon 44 (2006), pp. 778–785.

[37] M. Abdel-Goad and P. Potschke, *Rheological characterization of melt processed polycarbonate/multiwalled carbon nanotube composites*, J. Non-New. Fl. Mech. 128 (2005), pp. 2–6.

[38] R. Haggenmueller, H.H. Gommans, A.G. Rinzler, J.E. Fischer, and K.I. Winey, *Aligned single-wall carbon nanotubes in composites by melt processing methods*, Chem. Phy. Lett. 330 (2000), pp. 219–225.

[39] M. Sennet, E. Welsh, J.B. Wright, W.Z. Li, J.G. Wen, and Z.F. Ren, *Dispersion and alignment of carbon nanotubes in polycarbonate*, Appl. Phy. A: Mat. Sci. Proc. 76 (2003), p. 111.